Published in final edited form as:

J Muscle Res Cell Motil. 2015 October ; 36(4-5): 329–337. doi:10.1007/s10974-015-9420-6.

Cyclic mechanical strain of myocytes modifies CapZβ1 post translationally via PKCε

Ying-Hsi Lin[1], **Erik R. Swanson**[1], **Jieli Li**[1], **Michael A. Mkrtschjan**[1,2], and **Brenda Russell**[1,2]

[1]Department of Physiology and Biophysics, College of Medicine, University of Illinois at Chicago, MC 901, 835 S. Wolcott, Chicago, IL 60612, USA

[2]Department of Bioengineering, College of Engineering, University of Illinois at Chicago, Chicago, IL 60607, USA

Abstract

The heart is exquisitely sensitive to mechanical stimuli and adapts to increased demands for work by enlarging the cardiomyocytes. In order to determine links between mechano-transduction mechanisms and hypertrophy, neonatal rat ventricular myocytes (NRVM) were subjected to physiologic strain for analysis of the dynamics of the actin capping protein, CapZ, and its post-translational modifications (PTM). CapZ binding rates were assessed after strain by fluorescence recovery after photobleaching (FRAP) of green fluorescent protein (GFP) expressed by a GFP-CapZβ1 adenovirus. To assess the role of the protein kinase C epsilon isoform (PKCε), rest or cyclic strain were combined with specific PKCε activation by constitutively active PKCε, or by inhibition with dominant negative PKCε (dnPKCε) expression. Significant increases of CapZ FRAP kinetics with strain were blunted by dnPKCε, suggesting that PKCε is involved in mechano-transduction signaling. Similar combinations of strain and PKC regulation in NRVMs were studied by PTM profiles of CapZβ1 using quantitative two-dimensional gel electrophoresis. The significantly increased charge on CapZ seen with mechanical strain was reversed by the addition of dnPKCε. Potential clinical relevance was confirmed in vivo by PTMs of CapZ in the failing heart of one-year old transgenic mice over-expressing PKCε. Furthermore, with strain there was significant PKCε translocation to the Z-disc and co-localization with CapZβ1 or α-actinin, which was quantified on confocal images. A hypothetical model is presented proposing that one destination of the mechanotransduction signaling pathways might be for PTMs of CapZ thereby regulating actin capping and filament assembly.

Keywords

Actin capping; Sarcomere; Mechano-transduction; Mechano-signaling; Proteomics

Correspondence to: Brenda Russell.

Ying-Hsi Lin and Erik R. Swanson are co-first authors.

Electronic supplementary material The online version of this article (doi:10.1007/s10974-015-9420-6) contains supplementary material, which is available to authorized users.

Introduction

The heart is exquisitely sensitive to mechanical, hemodynamic, and hormonal stimuli, and adapts to increased demands for work by extensive remodeling. At the cellular level, cardiomyocytes are able to control both their size and shape in response to mechanical strain (Russell and Motlagh 1985). However, physiologic and pathologic mechanisms through which cardiomyocytes sense mechanical strain and respond by remodeling the sarcomeres and the actin cytoskeleton remain largely unknown. With abnormal mechanical cues from an underlying disease, the cells remodel disproportionally, leading to an inefficient, and ultimately failing heart. Early studies showed that the actin capping protein (CapZ) in the Z-disc regulated the polymerization of existing actin filaments (Maruyama 1966). Thus, one destination of the mechanotransduction signaling pathway might be to affect the post-translational modification (PTM) of CapZ, which controls actin capping and filament assembly.

CapZ is a heterodimeric protein (α and β subunits) capping the barbed end of the actin filament and slowing down its assembly (Cooper and Pollard 1985). An in vitro study showed that CapZ caps the actin filament dynamically and was highly regulated by several binding proteins and polyphosphoinositides (Li and Russell 2013; Taoka et al. 2003). In myocytes, CapZ and actin dynamics were increased very rapidly by hypertrophic stimulation, suggesting the possible involvement of PTMs in actin capping and filament assembly (Hartman et al. 2009; Li and Russell 2013; Lin et al. 2013).

Phosphorylation is critical in mechanotransduction signaling pathways. The protein kinase C isoform ε (PKCε) modulates both cardiac contractility and hypertrophic remodeling (Mochly-Rosen et al. 2000; Inagaki et al. 2002). When activated, PKCε translocates to the Z-disc (Disatnik et al. 1994; Robia et al. 2001). A dominant-negative mutant of PKCε prevents the assembly of the optimal resting length of the sarcomere after sustained mechanical strain, suggesting its regulatory role (Mansour et al. 2004). In a transgenic model of CapZ, PKC dependent myofilament function is abolished, and the binding of activated PKCε to the myofilament is diminished (Pyle et al. 2002), suggesting the involvement of CapZ in PKCε signaling. Furthermore, increased CapZ dynamics in neurohormonally stimulated myocytes regulate hypertrophy through PKCε and PIP_2 dependent pathways (Li and Russell 2013).

The goal of the present experiments is to investigate the mechanism by which CapZ dynamics is regulated by mechanical strain. The specific hypothesis tested is that CapZ undergoes a PKCε dependent PTM that affects its dynamics in response to mechanical strain. Neonatal rat ventricular myocytes (NRVM) were subjected to a brief period of physiologic mechanical strain with specific PKCε activation or inhibition. CapZ binding rates were assessed by FRAP of adenoviruses expressed GFP-CapZβ1. Furthermore, PTMs were assessed by 2D gel electrophoresis under the same conditions of strain PKCε activation or inhibition in NRVM. Confocal images showing translocation of PKCε were assessed by Fast Fourier Transform (FFT). To confirm the potential clinical relevance of these findings in the whole heart, CapZ PTMs were assessed in a heart failure model using ventricles from one-year old transgenic mice over-expressing PKCε (Hankiewicz et al. 2008).

Materials and methods

Cell culture

Primary heart cultures were obtained from neonatal rats according to Institutional Animal Care and Use Committee and NIH guidelines for the care and use of laboratory animals. Hearts were removed and cells isolated from 1 to 2 days old neonatal Sprague–Dawley rats and cultured at high density (1000 cells/mm^2) as previously described (Boateng et al. 2003).

Mechanical strain

Three days after cell isolation, with or without viral infection, NRVMs were strained at 10 % elongation biaxially at 1 Hz sinusoidally for 1 h with a Flexcell Strain Unit (model FX-4000, Flexcell International, Hillsborough, NC), as described previously (Boateng et al. 2003).

Adenoviral constructs and infection

Recombinant adenoviruses for GFP-CapZβ1, caPKCε and dnPKCε were kindly provided by Dr. Allen Samarel as previously described (Hartman et al. 2009). NRVMs were infected 2 days after isolation, with CapZβ1 (MOI 20), caPKCε (MOI 100), or dnPKCε (MOI 250) for 60 min at 37 °C diluted in PC-1 medium. These PKCε mutants were shown to be constitutively active or dominantly negative, respectively, by ^{32}P incorporation using a PKCε-specific peptide substrate (Strait et al. 2001). Viral medium was replaced with virus-free medium, and cells were left undisturbed for 20–24 h prior to use in the experiment.

FRAP for CapZ dynamics

FRAP has yielded qualitative and quantitative information about the processes that regulate actin polymerization in living myocytes. The methods and analysis for determining the GFP-CapZβ1 rate constant (K_{frap}) were previously described by us (Lin et al. 2013). Briefly, binding of CapZ to the actin filament has two binding states (Takeda et al. 2010), so FRAP curves of CapZ were fit using non-linear regression in OriginPro (OriginLab, Northampton, MA):

$$I_{frap}(t)=1-C_1e^{-Koff1t}-C_2e^{-Koff2t} \quad (1)$$

Koff1 an Koff2 represented the kinetic constants of the fast component and slow component, respectively. The average kinetic constant (K_{frap}) for dynamics was calculated using the following formula:

$$K_{frap}=C_1K_{off1}+C_2K_{off2} \quad (2)$$

Immunostaining and confocal microscopy

NRVMs were analyzed using standard methods (Mansour et al. 2004). Immunolabelling used primary anti-PKCε antibody (1:200) (Abcam, #ab63638) or α-actinin (Abcam, #ab9465), and secondary antibody (1:500) (Life Technologies, #A21202, Donkey anti-Mouse IgG (H+L) Secondary Antibody, Alexa Fluor® 488 conjugate, and #A21207,

Donkey anti-Rabbit IgG (H+L) Secondary Antibody, Alexa Fluor® 594 conjugate). The cytoskeleton remained after removal of membranes, cytosol, and nuclei and was observed by microscopy (Li and Russell 2013).

Quantification of translocation of PKCε to the Z-disc

Fluorescent imaging of unstrained and strained NRVM did a rigorous comparison of the subcellular location of PKCε. The Z-disc was identified in one series by GFP-CapZβ1 and in a second by α-actinin. Images of ten randomly selected cells in each series were captured with a Zeiss LSM 710 Confocal Microscope (META). Laser intensity and detector gain were set manually for the first images of both the GFP-CapZβ1 and α-actinin series and left unchanged for the remainder of the experiment, ensuring standardized readings in each cell. Using ImageJ, three line scans of 10 sarcomeres in each cell were chosen randomly for either the GFP-CapZβ1 or the α-actinin images, totaling 30 measured sarcomeres and approximately sixty microns line scan length per cell. Raw fluorescence intensities and positions of the line scan were recorded. Line scan positions were then translated to corresponding PKCε images and fluorescence intensity values were recorded. These data, which served as distance domain values, were imported into MATLAB for further analysis. Within MATLAB, the Fast Fourier Transform (FFT) function was used to convert distance domain to frequency domain. Thus, the first dominant FFT peak corresponded to the major sarcomeric periodicity and was used to determine the average sarcomere length for each cell. This was repeated for both the PKCε and GFP-CapZβ1 or the α-actinin images to test that localizations were occurring with the same sarcomere repeats. Additionally, intensity maxima within the distance domain of GFP-CapZβ1 or α-actinin were determined automatically and occurred at the Z-disc. Maxima positions were then translated to their corresponding PKCε distance domain fluorescence intensity values. Ratios of PKCε intensity to either GFP-CapZβ1 or α-actinin intensity at the Z-disc were calculated in order to compare control with strained myocytes.

Co-Immunoprecipitation

Cultured NRVM were washed twice in ice-cold PBS and lysed in RIPA buffer (50 mM Tris–HCl pH 7.4, 150 mM NaCl, 2 mM EDTA, 1 % NP40, 0.1 % SDS) plus phosphatase inhibitors (Sigma Aldrich, #P5726, P0044) for 1 h at 4 °C under constant agitation. Following protein extraction, protein lysates were precleared using 25 μl Protein A/G Plus-Agarose beads (Santa Cruz, #sc-2003) for 1 h at 4 °C. Precleared lysates were incubated 24 h with 2 μg of CapZβ1 antibody (Millipore, #AB6017) at 4 °C, then immunocomplexes were isolated by adding Protein A/G Plus-Agarose beads overnight at 4 °C. As a negative control, the precleared lysates had only the Protein A/G Plus-Agarose beads, with rabbit serum. As a positive control, the precleared lysates had only the Protein A/G Plus-Agarose beads, with α-actin antibody (Sigma, A4700). Beads were washed three times in the binding buffer. SDS-PAGE and Western blotting were performed using 12 % Mini-PROTEAN® TGX™ Gel (Bio-Rad Laboratories, #456–1044). Polyvinylidene difluoride (PVDF) membranes were incubated with PKCε primary antibody (Abcam, #ab63638), followed by horseradish peroxidase (HRP) secondary antibody (anti-rabbit or antimouse) for 1 h at room temperature. Proteins were finally treated with an ECL Plus kit and visualized with the aid of Image Lab (Bio-Rad Laboratories).

PTM analysis of two-dimensional gel electrophoresis (2DGE)

Immediately following mechanical strain, cells were placed on ice and lysed using ice-cold standard relaxing buffer (75 mM KCl, 10 mM Imidazole, 2 mM $MgCl_2$, 2 mM EDTA, 1 mM NaN_3). The insoluble pellet was resolubilized in urea-thiourea-chaps buffer (8 M Urea, 2 M Thiourea, 4 % Chaps). 100 μg of protein was precipitated using a 2D Cleanup Kit (GE Healthcare, Burr Ridge, IL) and subjected to isoelectric focusing on pH 4–7IPG strips. Strips were loaded on 12.5 % SDS–polyacrylamide gels and run at 30 mA per gel. Proteins were transferred to a PVDF membrane at 20 V for 70 min. Proteins were probed with CapZβ1 antibody (1:1000, mAb 1E5.25.4, Developmental Studies Hybridoma Bank, IA) and visualized using enhanced chemiluminescence (ECL+, Amersham, Arlington Heights, IL). Strips were scanned by Gel Doc™ XR+ and ChemiDoc™ XRS+ System and spots quantified by Image Lab^T Software. Spot intensity was recorded and single spot intensity was normalized as the % of the total intensity of all spots.

CapZ structure and PTM site prediction

CapZ structure was represented using PyMOL Molecular Graphics System. PTM phosphorylation charged sites for serine (S), threonine (T) and tyrosine (Y) on CapZ were predicted by NetPhos 2.0 (http://www.cbs.dtu.dk/services/NetPhos/) (Blom et al. 1999). Acetylation sites for lysine (K) were predicted using the PAIL algorithm (http://bdmpail.biocuckoo.org/prediction.php) (Li et al. 2006).

Failing mouse ventricular tissue

Tissue was collected from normal and transgenic PKCε overexpressing mice at 12 months of age and kindly provided by Dr. P Goldspink as described previously (Hankiewicz et al. 2008). Tissue samples were quickly frozen in liquid nitrogen in the operating room and stored at −80 °C. Three samples per each condition were used.

Statistics

Data are presented as mean ± SE. Sample number (n) for FRAP was defined as individual cells, with at least 3 separate cultures analyzed per experimental condition. FRAP curves were analyzed individually over time to account for any experimental variance. For 2DGE, sample number was defined as individual protein samples from at least 3 separate cultures or tissue samples. Statistical significance was determined using Student's *T* Test with significance taken at $P < 0.05$.

Results

CapZβ1 dynamics are altered by mechanical strain and regulated by PKCε

The FRAP recovery curves were generated by bleaching GFP-CapZβ1 (Fig. 1a). K_{frap} values for each of the conditions indicated altered binding dynamics of CapZβ1 after mechanical strain or treatment with caPKCε (Fig. 1b). Additionally, non-strained cells treated with caPKCε had a Kfrap, which was significantly higher than untreated, nonstrained cells, but not significantly different from strained cells. Strained cells treated with dnPKCε

had a K_{frap}, which was not significantly different from non-strained cells, but significantly decreased from strained and non-strained cells treated with caPKCε.

PTM of CapZβ1

This rapid response of CapZ dynamics to mechanical strain suggests that the alterations in dynamics are not caused by modified gene or protein expression, but rather through PTMs that act on existing proteins. 2DGE was used to assess any PTMs of CapZ after stimulation. Western blotting for CapZβ1 displayed three distinct spots of PTM (Fig. 2a). The three spots were identified at the expected molecular weight of CapZβ1 with isoelectric points of approximately 5.36, 5.24, and 5.13 corresponding to an uncharged form, a singly charged form, and a doubly charged form, respectively.

CapZβ1 post-translational profile is altered by mechanical strain in NRVM and involves PKCε

Treatment of NRVMs with mechanical strain, caPKCε, or mechanical strain and dnPKCε significantly altered the relative optical density of each CapZβ1 2DGE spot (Fig. 2b). In all spot comparisons, the significance was $P < 0.05$, $n = 3$. In non-strained cells, the relative abundance of the non-modified (spot 1), singly modified (spot 2), and doubly modified form (spot 3) was 21.6 ± 2.0, 49.2 ± 3.3, and 29.1 ± 4.7 %, respectively. In strained cells, the abundance of each form was significantly altered to 5.8 ± 0.6, 80.9 ± 1.9, and 13.3 ± 2.5 %. In non-strained cells treated with caPKCε, the abundance of each form was 4.2 ± 0.02, 84.1 ± 1.4, and 11.6 ± 1.4 %. Finally, in strained cells treated with dnPKCε, the abundance of each form was 35.9 ± 2.8, 32.6 ± 1.1, and 31.5 ± 1.7 %. Significant difference was observed in the abundance of the first form (spot 1) between non-strained controls and strained cells, and nonstrained cells and cells treated with caPKCε. Significant difference between the second from (spot 2) was noted between non-strained cells and strained cells, and nonstrained cells and cells treated with caPKCε; significant difference was also noted between non-strained cells treated with caPKCε and strained cells treated with dnPKCε.

CapZβ1 PTM profile is altered in failing transgenic mouse heart

Ventricular tissue from transgenic mice overexpressing a constitutively active form of PKCε exhibiting hypertrophy and heart failure at 12 months was compared with age matched non-transgenic mice (Hankiewicz et al. 2008). This 2DGE results displayed a significant difference in PTM profile (Fig. 2c, d). These whole heart results were taken together with the CapZ dynamics on NRVM, suggesting that PKCε alters the PTM profile of CapZβ1.

PKCε translocates to the sarcomere and colocalizes with CapZβ1 following mechanical strain

Since PKCε translocates to the sarcomere in hypertrophic myocytes, it is possible that PKCε phosphorylates CapZ and directly or indirectly alters its capping properties. Thus, distribution of PKCε was determined under the experimental conditions of cyclic strain. Quantified fluorescence intensity for PKCε to α-actinin ratio in the strained cells showed significantly higher levels in the strained NRVMs, $P < 0.00001$, $n = 10$ cells (Fig. 3a, c, e). Additionally, more PKCε colocalized with GFP-CapZβ1 in strained cells, compared with

non-strained NRVMs, $P < 0.0001$, $n = 10$ (Fig. 3b, d, f), suggesting the translocation of PKCε to the Z-disc with one hour of cyclic strain. The periodicity of colocalized of PKCε with CapZ or α-actinin was further quantified by Fast Fourier Transform to determine the sarcomere length, which showed no significant differences between the periodicity in control or strained NRVM (Supplemental Tables 1, 2). Thus, the translocated PKCε was also sarcomeric with maxima at the Z-disc identified by either α-actinin or CapZ. Furthermore, coimmunoprecipitation showed a direct interaction between CapZβ1 and PKCε (Fig. 3g).

Discussion

Here, we observed for the first time that mechanical strain regulated (1) PTMs of CapZβ1 (2) FRAP rate constant dynamics of CapZβ1 in a PKCε dependent manner, and (3) translocation of PKCε to the Z-disc where it colocalized with a- actinin and CapZβ1. Interestingly, we found that heart failure tissue from a transgenic mouse overexpressing PKCε had similar PTMs of CapZβ1, suggesting possible clinical relevance. The negative charge shifts on CapZ suggest the PTMs are due to phosphorylation of serine (S), tyrosine (Y) or threonine (T) or to the acetylation of lysine (K) amino acids. The mechanism to alter actin capping activity may depend on increased charge directly modifying the secondary structure of CapZ at the predicted phosphorylation sites (Y111, Y107, S160, S161, S204, S207, S263, or T267) or acetylated sites (K159, K199 or K256) located at the interface between the CapZ and the barbed end of the actin filaments (Fig. 4a) (Hartman et al. 2009). In experimental PTM site screening, various phosphorylation sites on CapZβ1 have been identified (phosphosite.org database). Also, CapZβ1 can be acetylated in multiple spots as determined by mass spectrometry scanning (Lundby et al. 2012). However, the functional effects of these PTMs on actin assembly have not been addressed. Based on our novel findings, a hypothetical diagram proposes a molecular mechanism by which conformational structural changes to CapZ by PTMs alters its binding to the barbed end of the actin filament, thereby regulating actin capping and filament assembly (Fig. 4b).

CapZβ1 responds to neurohormonal and mechanical mechanosensing pathways and integrates their signals as we and others have suggested (Hartman et al. 2009; Li and Russell 2013; Li et al. 2014; Lin et al. 2013). CapZ dynamics are closely correlated with actin dynamics and sarcomere assembly, thus linking the CapZ capping process to cardiac hypertrophy. Potential interaction between active PKCε and CapZ and subsequent uncapping may explain the observation of decreased amounts of active PKCε in the myofilament fraction of CapZβ1 downregulated murine hearts (Pyle et al. 2002). Mechanical strain initiates an IP3/DAG pathway that generates active PKCε (Bullard et al. 2007). Furthermore, the PTM mechanism proposed here is supported by our earlier findings of an increased uncapping rate with stimulation of mechanical strain (Li and Russell 2013; Lin et al. 2013).

Both the CapZα and CapZβ monomers have C-terminal tentacles that stabilize binding of the CapZ heterodimeric cap to actin (Takeda et al. 2010). Binding to the β tentacle alone allows it to wobble (Kim et al. 2010) and expose additional binding sites on the actin interface that may bind CapZ inhibitory or dissociation proteins (Schafer et al. 1996; Takeda et al. 2010). The C-terminal tentacles of the alpha and beta subunits are amphiphilic and

contain both a strongly hydrophobic actin-binding region, and a hydrophilic region capable of binding partnering proteins (Yamashita et al. 2003). The accessible hydrophobic charge present at the Z-disc when CapZ is bound in its wobble state may promote partnering with proteins containing hydrophobic binding regions such as PKCε, V-1/myotrophin, PIP_2, and others (Bhattacharya et al. 2006). For example, the structure of PKCε contains a C-1 region capable of binding hydrophobic surfaces (Zhang et al. 1995). One such location could be on the beta tentacle, since its deletion affects actin assembly after a short bout of exercise (Lin et al. 2013). Translocation of PKCε to the sarcomere resulted in cardiac hypertrophy with a thin ventricular wall (Mochly-Rosen et al. 2000). Colocalization is confirmed here for PKCε with either α-actinin or CapZβ1 in mechanically strained myocytes (Fig. 3).

It is tempting to assume that the charge modification seen is due to direct phosphorylation of CapZ by PKCε but it could be indirect through some additional binding partner, or by generating byproducts capable of dissociating CapZ from actin. Charge modification of proteins also occurs with acetylation. Myofibrillar protein acetylation/ deacetylation is mediated by HDACs and has been linked to the generation of cardiac remodeling induced by pressure overload and neurohormonal stimulation (Demos-Davies et al. 2014; Gupta et al. 2008; Samant et al. 2015). Phosphorylation by PKCε/PKD plays a regulatory role in cardiac hypertrophy involving Class IIa HDACs (Monovich et al. 2010). One can further speculate that PKCε and HDAC signaling may interact directly. Furthermore, some PTMs cannot be measured by 2DGE because they are not associated with charge change, such as methylation or oxidation. For example, CapZ and actin dynamic regulation does occur without charge change or PTM by PIP_2 involvement in actin capping (Hartman et al. 2009; Li and Russell 2013; Li et al. 2014). Thus, numerous signaling pathways could contribute to the regulation of CapZ and cardiac hypertrophy.

The causes of altered CapZβ1 dynamics are still largely unknown, but they are not likely to result from alterations in gene and protein expression level, which take many hours to establish, whereas PTMs and protein dynamics are rapid. The increased dynamic properties of CapZ reflect its enhanced uncapping rate and loosening from the actin filament possibly because of PTMs in the actin binding region. However, increased dynamics did not lead to a diffused localization of CapZ. Therefore, it is possible that other partnering proteins, such as α- actinin (Papa et al. 1999), anchor CapZ at sites away from the actin binding surface. Changes in actin capping in situations of increased load may support clinical findings of cardiomyopathies and constitutively active PKCα overexpression in transgenic animals and cells (Hankiewicz et al. 2008; Strait et al. 2001). This report is an initial step towards a better understanding about PTM of this crucial actin capping protein in adaptation to physiologic exercise and in pathologic heart disease.

Acknowledgments

We thank Allen M. Samarel (Loyola University Chicago Stritch School of Medicine, Maywood, IL) for the gift of the CapZ and PKCε DNA constructs. Normal and transgenic PKCε overexpressing mouse ventricles were kindly provided by Dr. Paul Goldspink from tissue stored at UIC. This work was supported by NIH HL-62426 (BR) and American Heart Association 12PRE12050371 (Y.-H. Lin).

References

Bhattacharya N, Ghosh S, Sept D, Cooper JA. Binding of myotrophin/V-1 to actin-capping protein: implications for how capping protein binds to the filament barbed end. J Biol Chem. 2006; 281(41): 31021–31030. [PubMed: 16895918]

Blom N, Gammeltoft S, Brunak S. Sequence and structure-based prediction of eukaryotic protein phosphorylation sites. J Mol Biol. 1999; 294(5):1351–1362. [PubMed: 10600390]

Boateng SY, Hartman TJ, Ahluwalia N, Vidula H, Desai TA, Russell B. Inhibition of fibroblast proliferation in cardiac myocyte cultures by surface microtopography. Am J Physiol Cell Physiol. 2003; 285(1):C171–C182. [PubMed: 12672651]

Bullard TA, Hastings JL, Davis JM, Borg TK, Price RL. Altered PKC expression and phosphorylation in response to the nature, direction, and magnitude of mechanical stretch. Can J Physiol Pharmacol. 2007; 85(2):243–250. [PubMed: 17487266]

Cooper JA, Pollard TD. Effect of capping protein on the kinetics of actin polymerization. Biochemistry. 1985; 24(3):793–799. [PubMed: 3994986]

Demos-Davies KM, Ferguson BS, Cavasin MA, Mahaffey JH, Williams SM, Spiltoir JI, Schuetze KB, Horn TR, Chen B, Ferrara C, Scellini B, Piroddi N, Tesi C, Poggesi C, Jeong MY, McKinsey TA. HDAC6 contributes to pathological responses of heart and skeletal muscle to chronic angiotensin-II signaling. Am J Physiol Heart Circ Physiol. 2014; 307(2):H252–H258. [PubMed: 24858848]

Disatnik MH, Buraggi G, Mochly-Rosen D. Localization of protein kinase C isozymes in cardiac myocytes. Exp Cell Res. 1994; 210(2):287–297. [PubMed: 8299726]

Gupta MP, Samant SA, Smith SH, Shroff SG. HDAC4 and PCAF bind to cardiac sarcomeres and play a role in regulating myofilament contractile activity. J Biol Chem. 2008; 283(15):10135–10146. [PubMed: 18250163]

Hankiewicz JH, Goldspink PH, Buttrick PM, Lewandowski ED. Principal strain changes precede ventricular wall thinning during transition to heart failure in a mouse model of dilated cardiomyopathy. Am J Physiol Heart Circ Physiol. 2008; 294(1):H330–H336. [PubMed: 17965277]

Hartman TJ, Martin JL, Solaro RJ, Samarel AM, Russell B. CapZ dynamics are altered by endothelin-1 and phenylephrine via PIP2- and PKC-dependent mechanisms. Am J Physiol Cell Physiol. 2009; 296(5):C1034–C1039. [PubMed: 19295171]

Inagaki K, Iwanaga Y, Sarai N, Onozawa Y, Takenaka H, Mochly-Rosen D, Kihara Y. Tissue angiotensin II during progression or ventricular hypertrophy to heart failure in hypertensive rats; differential effects on PKC epsilon and PKC beta. J Mol Cell Cardiol. 2002; 34(10):1377–1385. [PubMed: 12392998]

Kim T, Cooper JA, Sept D. The interaction of capping protein with the barbed end of the actin filament. J Mol Biol. 2010; 404(5):794–802. [PubMed: 20969875]

Li J, Russell B. Phosphatidylinositol 4,5-bisphosphate regulates CapZβ1 and actin dynamics in response to mechanical strain. Am J Physiol Heart Circ Physiol. 2013; 305(11):H1614–H1623. [PubMed: 24043251]

Li A, Xue Y, Jin C, Wang M, Yao X. Prediction of Nepsilonacetylation on internal lysines implemented in Bayesian discriminant method. Biochem Biophys Res Commun. 2006; 350(4): 818–824. [PubMed: 17045240]

Li J, Tanhehco EJ, Russell B. Actin dynamics is rapidly regulated by the PTEN and PIP2 signaling pathways leading to myocyte hypertrophy. Am J Physiol Heart Circ Physiol. 2014; 307(11):H1618–H1625. [PubMed: 25260617]

Lin YH, Li J, Swanson ER, Russell B. CapZ and actin capping dynamics increase in myocytes after a bout of exercise and abates in hours after stimulation ends. J Appl Physiol. 2013; 114(11):1603–1609. [PubMed: 23493359]

Lundby A, Lage K, Weinert BT, Bekker-Jensen DB, Secher A, Skovgaard T, Kelstrup CD, Dmytriyev A, Choudhary C, Lundby C, Olsen JV. Proteomic analysis of lysine acetylation sites in rat tissues reveals organ specificity and subcellular patterns. Cell Rep. 2012; 2(2):419–431. [PubMed: 22902405]

Mansour H, de Tombe PP, Samarel AM, Russell B. Restoration of resting sarcomere length after uniaxial static strain is regulated by protein kinase Cepsilon and focal adhesion kinase. Circ Res. 2004; 94(5):642–649. [PubMed: 14963000]

Maruyama K. Effect of beta-actinin on the particle length of F-actin. Biochim Biophys Acta. 1966; 126(2):389–398. [PubMed: 5971860]

Mochly-Rosen D, Wu G, Hahn H, Osinska H, Liron T, Lorenz JN, Yatani A, Robbins J, Dorn GW 2nd. Cardiotrophic effects of protein kinase C epsilon: analysis by in vivo modulation of PKCepsilon translocation. Circ Res. 2000; 86(11):1173–1179. [PubMed: 10850970]

Monovich L, Vega RB, Meredith E, Miranda K, Rao C, Capparelli M, Lemon DD, Phan D, Koch KA, Chapo JA, Hood DB, McKinsey TA. A novel kinase inhibitor establishes a predominant role for protein kinase D as a cardiac class IIa histone deacetylase kinase. FEBS Lett. 2010; 584(3):631–637. [PubMed: 20018189]

Papa I, Astier C, Kwiatek O, Raynaud F, Bonnal C, Lebart MC, Roustan C, Benyamin Y. Alpha actinin-CapZ, an anchoring complex for thin filaments in Z-line. J Muscle Res Cell Motil. 1999; 20(2):187–197. [PubMed: 10412090]

Pyle WG, Hart MC, Cooper JA, Sumandea MP, de Tombe PP, Solaro RJ. Actin capping protein: an essential element in protein kinase signaling to the myofilaments. Circ Res. 2002; 90(12):1299–1306. [PubMed: 12089068]

Robia SL, Ghanta J, Robu VG, Walker JW. Localization and kinetics of protein kinase C-epsilon anchoring in cardiac myocytes. Biophys J. 2001; 80(5):2140–2151. [PubMed: 11325717]

Russell B, Motlagh D. Ashley WW (2000) Form follows function: how muscle shape is regulated by work. J Appl Physiol. 1985; 88(3):1127–1132.

Samant SA, Pillai VB, Sundaresan NR, Shroff SG, Gupta MP. Histone deacetylase 3 (HDAC3)-dependent reversible lysine acetylation of cardiac myosin heavy chain isoforms modulates their enzymatic and motor activity. J Biol Chem. 2015; 290(25):15559–15569. [PubMed: 25911107]

Schafer DA, Jennings PB, Cooper JA. Dynamics of capping protein and actin assembly in vitro: uncapping barbed ends by polyphosphoinositides. J Cell Biol. 1996; 135(1):169–179. [PubMed: 8858171]

Strait JB 3rd, Martin JL, Bayer A, Mestril R, Eble DM, Samarel AM. Role of protein kinase C-epsilon in hypertrophy of cultured neonatal rat ventricular myocytes. Am J Physiol Heart Circ Physiol. 2001; 280(2):H756–H766. [PubMed: 11158975]

Takeda S, Minakata S, Koike R, Kawahata I, Narita A, Kitazawa M, Ota M, Yamakuni T, Maéda Y, Nitanai Y. Two distinct mechanisms for actin capping protein regulationsteric and allosteric inhibition. PLoS Biol. 2010; 8(7):e1000416. [PubMed: 20625546]

Taoka M, Ichimura T, Wakamiya-Tsuruta A, Kubota Y, Araki T, Obinata T, Isobe T. V-1, a protein expressed transiently during murine cerebellar development, regulates actin polymerization via interaction with capping protein. J Biol Chem. 2003; 278(8):5864–5870. [PubMed: 12488317]

Yamashita A, Maeda K, Maéda Y. Crystal structure of CapZ: structural basis for actin filament barbed end capping. EMBO J. 2003; 22(7):1529–1538. [PubMed: 12660160]

Zhang G, Kazanietz MG, Blumberg PM, Hurley JH. Crystal structure of the cys2 activator-binding domain of protein kinase C delta in complex with phorbol ester. Cell. 1995; 81(6):917–924. [PubMed: 7781068]

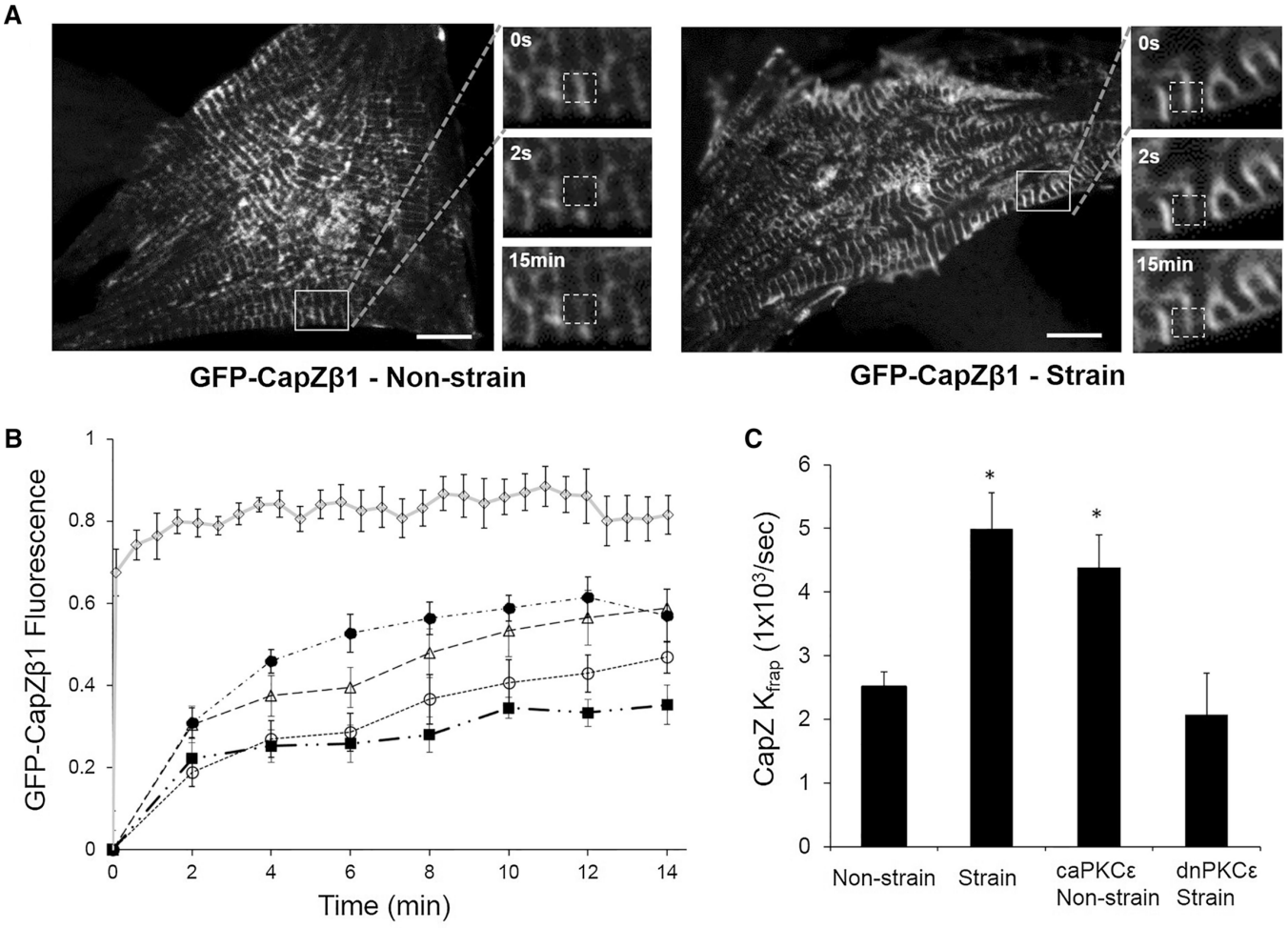

Fig. 1.

PKCε regulates CapZβ1 dynamics of myocytes after mechanical strain. NRVMs were infected with the GFP-CapZβ1 fusion protein with or without caPKCε or dnPKCε viral incubated for 1 h then for exchanged with non-viral media for 24 h. NRVMs were cyclically strained at 10 % for 1 h, followed immediately by the experiments: **a** Striations are seen with GFP-CapZβ1 infection in strained and non-strained myocytes at lower magnification. *Scale bar* 10 μm. Inset: higher magnification images of area delineated by the solid white boxes containing the smaller region of interest (ROI) shown as a *dashed white box* (3.75 × 3.75 μm) at time before bleaching (0 s), full bleach (2 s later) and 15 min to show fluorescent recovery after photo bleaching (FRAP). **b** Time course used for K_{frap} analysis on cells expressing the GFP-CapZβ1 fusion protein. *Open circle* non-strain (n = 7); *closed circle* 1 h strain (n = 7); *open triangle* caPKCε/non-strain (n = 7); *closed square* dnPKCε/strain (n = 4); *open diamond* GFP only (n = 5). **c** K_{frap} values for GFP-CapZβ1. Mean ± SEM (*P < 0.05 vs. non-strain)

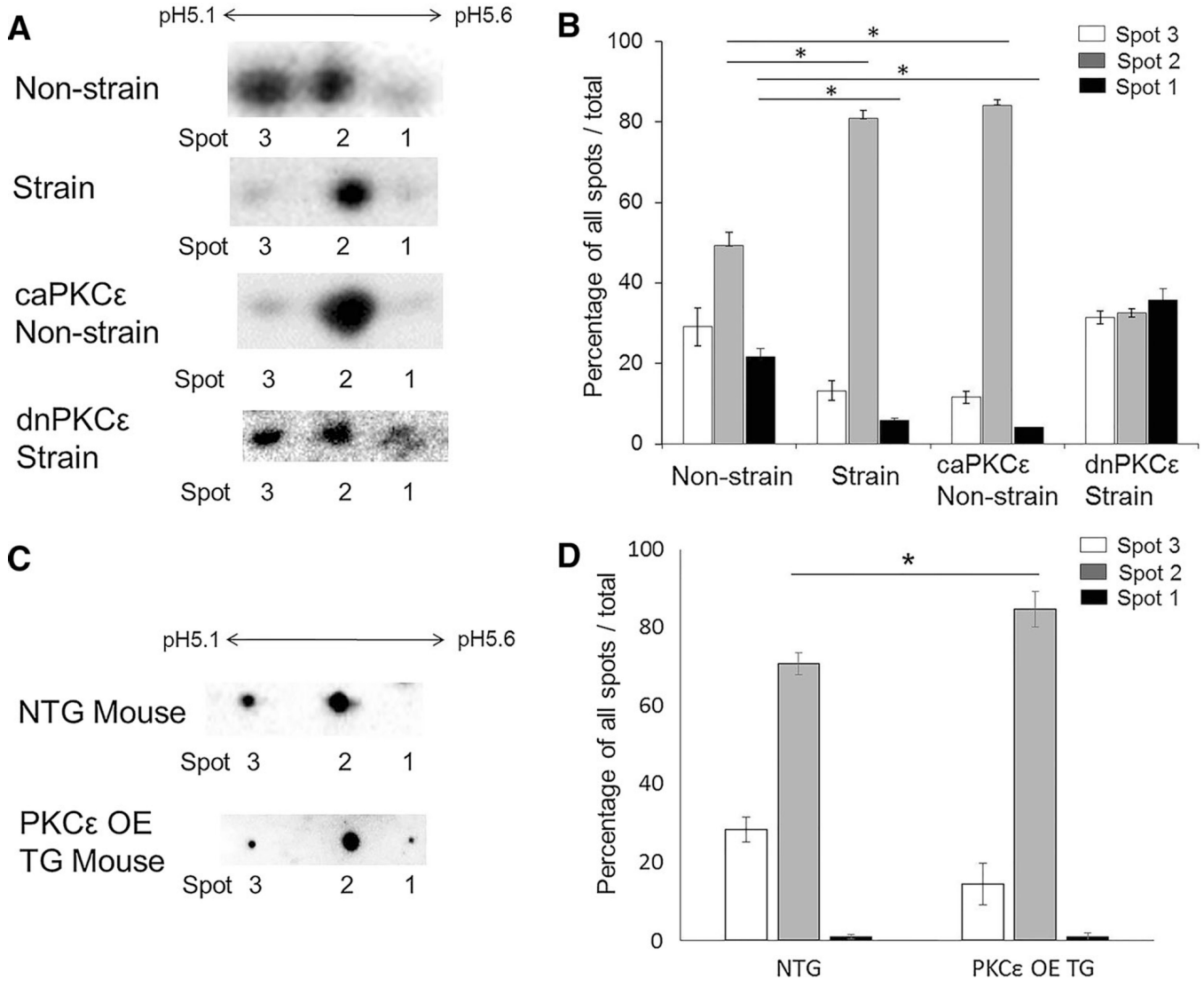

Fig. 2.

The post-translational profile of endogenous CapZβ1 changes in response to mechanical strain and involves PKCε. **a, b** Immediately after strain, with or without caPKCε or dnPKCε, NRVMs were lysed for 2D gel electrophoresis and immunodetection with a CapZβ1 antibody. Three distinct PTM spots were detected for CapZβ1 at ~31 kDa and pI of ~5.36, ~5.24, and ~5.13. Histogram of relative spot intensities shows mechanical strain with caPKCε treatment alters the CapZβ1 PTM profile relative to non-strained controls (*P < 0.05, n = 3). **c, d** In ventricular tissue from one year-old non-transgenic or transgenic mice overexpressing caPKCε, two distinct CapZβ1 PTM spots at ~31 kDa have varied intensities, with pI of ~5.24, and ~5.13 corresponding to spots 2 and 3 of NRVMs. Histogram of relative intensities shows PKCε overexpression alters the PTM relative to age matched control tissue (*P < 0.05, n = 3)

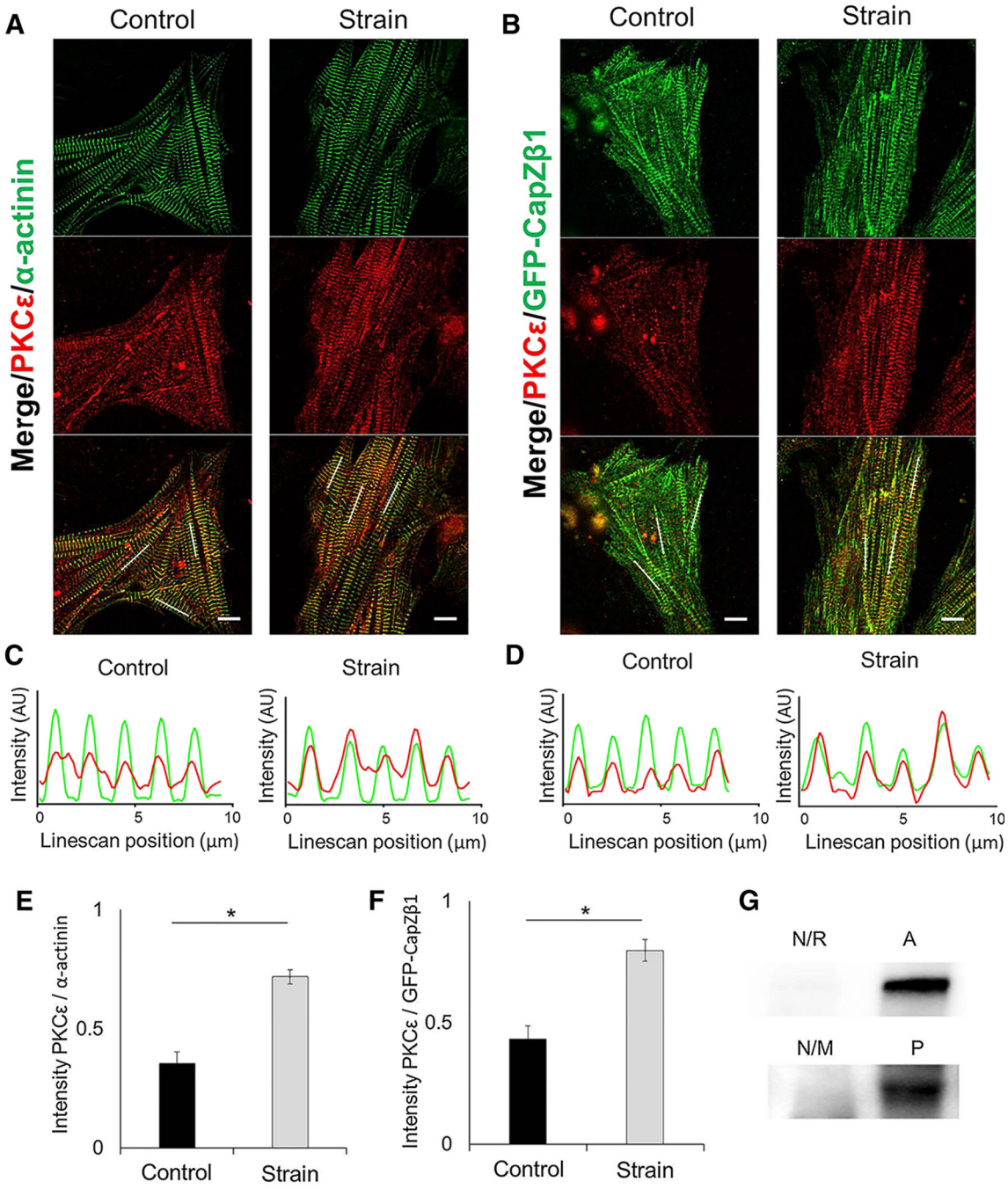

Fig. 3.

PKCε co-localization with α-actinin or CapZβ1 increases at the Z-disc after cyclic strain of neonatal ventricular cardiac myocytes. Myocytes were unstrained (control) or cyclically strained for 1 h at 10 % (strain) followed by confocal imaging for **a** PKCε (*red*, antibody staining) with α-actinin (*green*, antibody staining), or **b** PKCε (*red*, antibody staining) and GFP-CapZβ1 (*green* fluorescence). Note that only the cytoskeletal fraction remained after removal of the cytosol, membrane organelles and nuclei. **c, d** Higher co-localization was seen in the strained than in the non-strained myocytes in line scans indicated by white lines

(10 sarcomere repeats per scan, 3 line scans per cell). Little PKCε was seen in unstrained cells but there was a significant increase at the Z-disc after I hour of 10 % cyclic strain. **e** Histogram for quantification under each condition showed increased co-localization of PKCε with α-actinin in the strained myocytes, n = 10 cells, $P < 0.00001$. **f** Histogram for quantification of increased co-localization of PKCε with GFP-CapZβ1 in the strained myocytes, n = 10 cells, $P < 0.0001$. **g** Co-immunoprecipitation of CapZβ1 and PKCε. N/R: IgA/G beads with rabbit serum; A: IgA beads with CapZβ1 antibody; N/M: IgA/G beads with rabbit serum; *P* positive control, IgA/G beads with α-actin antibody. (Color figure online)

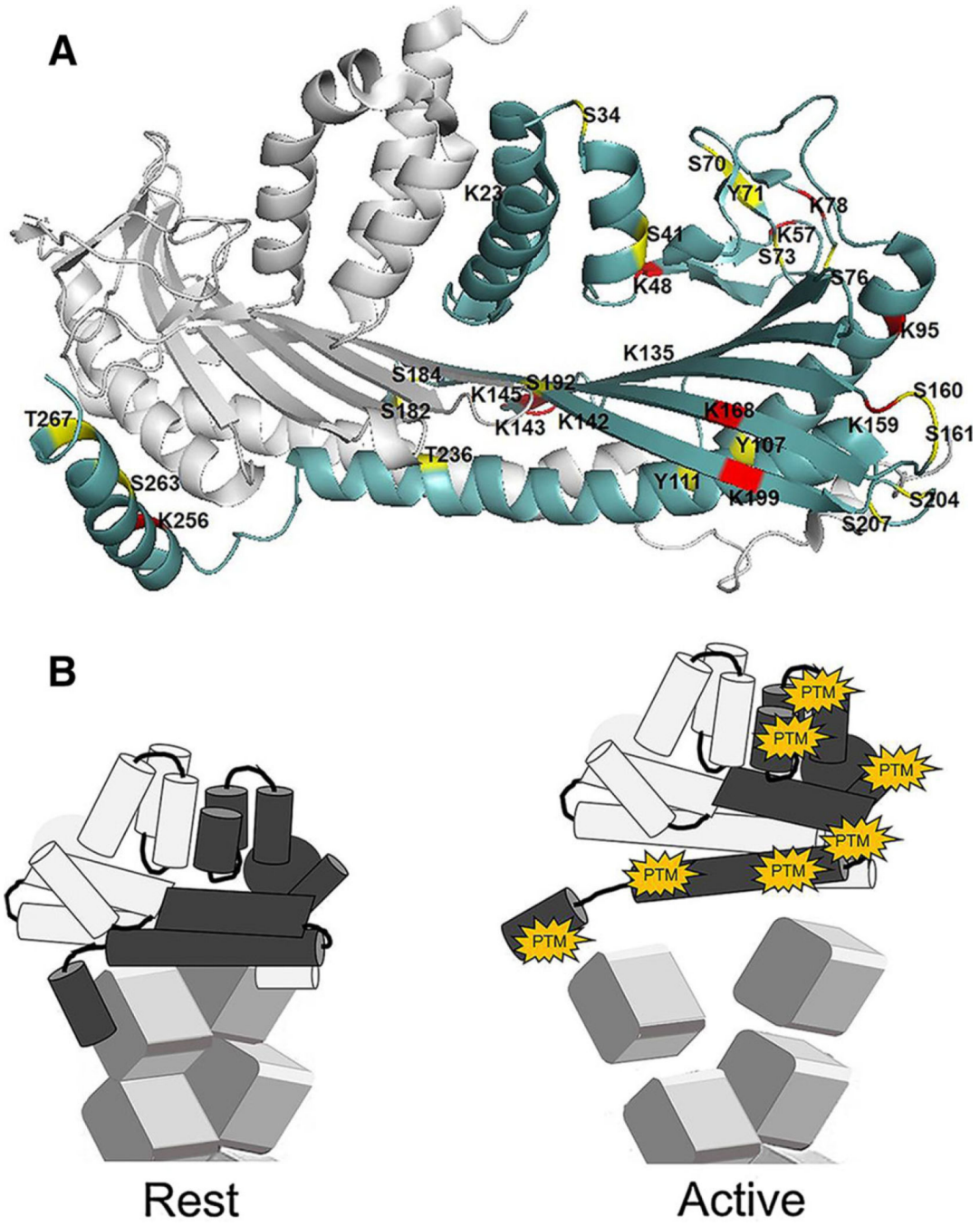

Fig. 4.

Model for CapZ PTM regulation of actin assembly. **a** CapZ structure and potential PTM sites. *Light grey* CapZα1; *light blue* CapZβ1; *yellow* predicted phosphorylation sites; *red* predicted acetylation sites. **b** During rest, PTM levels of CapZ are low and the interaction of CapZ with the actin filament is strong. With mechanical strain or exercise, PTMs on the actin binding of CapZβ1 interface are hypothesized to cause a conformational change,

lowering the binding affinity of CapZ to the barbed end of the actin filaments. The off rate of actin is elevated and actin assembly is increased. (Color figure online)